

Interpretable modeling for short- and medium-term electricity load forecasting

Kei Hirose ^{1,2}

¹ Institute of Mathematics for Industry, Kyushu University, 744 Motooka, Nishi-ku, Fukuoka 819-0395, Japan

² RIKEN Center for Advanced Intelligence Project, 1-4-1 Nihonbashi, Chuo-ku, Tokyo 103-0027, Japan

E-mail: hirose@imi.kyushu-u.ac.jp

Abstract

We consider the problem of short- and medium-term electricity load forecasting by using past loads and daily weather forecast information. Conventionally, many researchers have directly applied regression analysis. However, interpreting the effect of weather on these loads is difficult with the existing methods. In this study, we build a statistical model that resolves this interpretation issue. A varying coefficient model with basis expansion is used to capture the nonlinear structure of the weather effect. This approach results in an interpretable model when the regression coefficients are nonnegative. To estimate the nonnegative regression coefficients, we employ nonnegative least squares. Real data analysis shows the practicality of our proposed statistical modeling. The interpretation would be helpful for making strategies for energy-saving intervention and demand response.

Key Words: basis expansion; nonnegative least squares; short-term load forecasting; varying coefficient model

1 Introduction

Short- and medium-term load forecasting with high accuracy is essential for decision making during trade in electricity markets. In the past several decades, many forecasting methods have been proposed in literature. The forecasting techniques are mainly classified into two categories: machine learning approaches and statistical approaches. The machine learning techniques for example, support vector regression (Elattar et al., 2010;

Chen et al., 2017; Jiang et al., 2018), neural networks (He, 2017; Kong et al., 2018; Guo et al., 2018b; Bedi and Toshniwal, 2019), and hybrid of multiple forecasting techniques (Cho et al., 2013; Miswan et al., 2016; Liu et al., 2017; de Oliveira and Oliveira, 2018), have attracted attention in recent years. These techniques capture complex nonlinear structures; therefore, high forecast accuracy is expected.

Meanwhile, statistical approaches have also been extensively studied. Traditional statistical approaches include linear regression (Amral et al., 2008; Dudek, 2016; Saber and Alam, 2017), smoothing spline (Engle et al., 1986; Harvey and Kopman, 1993), autoregressive integrated moving average (ARIMA, Lee and Ko, 2011), and Kalman filter (Amjady, 2001). Recently, several authors have applied functional data analysis, where the daily curves of electricity loads are expressed as functions (Cabrera and Schulz, 2017; Vilar et al., 2018). Most of the statistical approaches are based on probabilistic forecasts, which lead to construction of the forecast interval. The distribution of the forecast values is helpful for risk management (Cabrera and Schulz, 2017). Reviews of the probabilistic forecasts were carried out by Hong and Fan (2016); van der Meer et al. (2018).

To forecast the loads, we usually use past loads, weather, and other factors as exploratory variables (e.g., Lusi et al., 2017). In practice, the time intervals are different among exploratory variables. For example, assume we forecast loads for a day that is a few days after today at 30-minute intervals; this is a common scenario for market transactions in electricity exchanges (e.g., the day-ahead market in the European Power Exchange, EPEX). The electricity loads are collected at 30-minute intervals using a smart meter, whereas weather forecast information, such as maximum temperature and average humidity, is usually observed at intervals of one day. Thus, this study uses past loads at 30-minute intervals and daily weather forecast information as exploratory variables. The other variables, such as the interior environment of buildings (e.g., Yildiz et al., 2017), may improve the accuracy but are not used in this study in order to illustrate a basic idea. Our proposed method, which will be described later, is able to directly incorporate the other variables.

From a suppliers' point of view, it is crucial to produce an interpretable model to investigate the impact of weather on the loads. For example, estimating the amount of electricity fluctuations caused by weather would be helpful for making strategies for

energy-saving intervention (e.g., Guo et al., 2018a; Wang et al., 2018) and demand response (e.g., Ruiz-Abellón et al., 2020). To produce an interpretable model, it seems one can directly add weather forecast information to the exploratory variables in the regression model (Hong et al., 2010) and investigate the estimator of regression coefficients. More generally, techniques for interpreting any black-box model, including the deep neural networks, have been recently proposed, for example, Local Interpretable Model-agnostic Explanations (LIME) (Ribeiro et al., 2016) and SHapley Additive exPlanations (SHAP) (Lundberg and Lee, 2017). However, these methods are used for variable selection, i.e., a set of variables that plays an essential role in the forecast is selected. The variable selection cannot estimate the amount of electricity fluctuations caused by weather.

In contrast to variable selection, decomposition of the electricity load at time t , say y_t , into two parts is useful for interpretation:

$$y_t \approx \mu_t + b_t, \tag{1}$$

where μ_t and b_t are the effects of past loads and weather forecast information, respectively. Typically, we use loads at the same time interval of the previous days as exploratory variables (e.g., Lusi et al., 2017), and regression analysis is separately conducted on each time interval. We then construct estimators of μ_t and b_t , say $\hat{\mu}_t$ and \hat{b}_t , respectively. The interpretation is carried out by plotting a curve of \hat{b}_t . However, without elaborate construction and estimation of b_t , we face two issues.

The first issue is that the curve of \hat{b}_t often becomes non-smooth at any time interval (i.e., every 30 minutes) in our experience. The non-smooth daily curve of b_t is unrealistic because it implies the impact of *daily* weather forecast on loads changes non-smoothly every 30 minutes. This problem is caused by the fact that the regression analysis is separately conducted at each time interval. To address this issue, we should estimate parameters under the assumption that b_t is smooth.

The second issue is related to the parameter estimation procedure. In many cases, the regression coefficients are estimated through the least squares method. In our experience, however, the estimate of regression coefficients related to b_t can be negative. The negative regression coefficients lead to a negative value of \hat{b}_t . Since \hat{b}_t is the amount of electricity fluctuations caused by weather, the interpretation becomes unclear. To alleviate this

problem, we need to restrict the regression coefficients associated with b_t to nonnegative values.

In this study, we develop a statistical model that elaborately captures the nonlinear structure of daily weather information to address two challenges, as mentioned earlier. We employ the varying coefficient model (Hastie and Tibshirani, 1993; Fan and Zhang, 1999) with basis expansion, where the regression coefficients associated with weather are assumed to be different depending on the time intervals. The regression coefficients are expressed by a nonlinear smooth function with basis expansion, which allows us to generate a smooth function of \hat{b}_t . Furthermore, the weather effect \hat{b}_t is also expressed as a nonlinear smooth function. To generate nonnegative regression coefficients, we employ the nonnegative least squares (NNLS, e.g., Lawson and Hanson, 1995) estimation. NNLS estimates parameters under the constraint that all regression coefficients are nonnegative. With the NNLS estimation, the value of \hat{b}_t is always nonnegative; thus, the interpretation becomes clear. The proposed statistical modeling is applied to actual electricity load data on a research facility. The results show that our proposed model is able to produce an interpretable weather effect. Moreover, the forecast accuracy of our proposed model is comparable to (slightly better than) some existing methods.

The remainder of this paper is organized as follows: Section 2 describes our proposed model based on the varying coefficient model. In Section 3, we present the parameter estimation via nonnegative least squares. Section 4 presents the analysis of actual electricity load data. Concluding remarks are given in Section 5. Some technical proofs are deferred to the Appendices.

2 Proposed model

Short- and medium-term forecasting is often used for trading electricity in the market. Among various electricity markets, the day-ahead (or spot) and the intraday markets are popular in electricity exchanges, including the European Power Exchange (EPEX) (<https://www.epexspot.com/en/market-data/dayaheadauktion>) and Japan Electric Power Exchange (JEPX) (<http://www.jepx.org/english/index.html>). In the day-ahead market, contracts for the delivery of electricity on the following day are made. In

the intraday market, the power will be delivered several tens of minutes (e.g., 1 hour in JEPX) after the order is closed. In both markets, transactions are typically made in 30-minute intervals; thus, the suppliers must forecast the loads in 30-minute intervals. In this study, we consider the problem of forecasting loads that can be applied to both day-ahead and intraday markets.

Let y_{ij} be the electricity load at j th time interval on i th date ($i = 1, \dots, n, j = 1, \dots, J$). Typically, $J = 48$, because we usually forecast the loads in 30-minute intervals. We consider the following model:

$$y_{ij} = \mu_{ij} + b_{ij} + \varepsilon_{ij}, \tag{2}$$

where μ_{ij} is the effect of past electricity load, b_{ij} is the effect of weather, such as temperature and humidity, and ε_{ij} are error terms with $E[\varepsilon_{ij}] = 0$.

Typically, the error variances in the daytime are larger than those at midnight because of the uncertainty of human behavior in the daytime. Therefore, it would be reasonable to assume that $V[\varepsilon_{ij}] = \sigma_j^2$, i.e., the error variances depend on the time interval. One may assume the correlation of errors for different time intervals, i.e., $\text{Cor}(\varepsilon_{ij}, \varepsilon_{ij'}) \neq 0$ for some $j \neq j'$; however, the number of parameters becomes large. For this reason, we consider only the case where the errors are uncorrelated. Note that the final implementation of our proposed procedure described later is independent of the assumption of the correlation structure in errors.

One can express b_{ij} and μ_{ij} as linear or nonlinear functions of predictors and conduct the linear regression analysis. With this procedure, however, we face two issues, as mentioned in the introduction; thus, we carefully construct appropriate functions of b_{ij} and μ_{ij} .

2.1 Expression of b_{ij}

Weather forecast information is typically observed at intervals of one day and not 30 minutes (e.g., the maximum temperature of average humidity). For this reason, we assume that the weather forecast information does not depend on j . Let a vector of weather information be \mathbf{s}_i . We express b_{ij} as a function of \mathbf{s}_i . Here, we assume two structures as follows:

- It is well known that the relationship between weather variables and consumption is nonlinear. For example, the relationship between maximum temperature and consumption is approximated by a quadratic function (e.g., Hong et al., 2010) because air conditioners are used on both hot and cold days. For this reason, it is assumed that b_{ij} is expressed as some nonlinear function of \mathbf{s}_i .
- Although \mathbf{s}_i does not depend on j , the effect of weather, b_{ij} , may depend on j . For example, consumption in the daytime is affected by the maximum temperature more than that at midnight. In this case, the regression coefficients associated with \mathbf{s}_i change according to the time interval j . However, if we assume different parameters at each time interval, the number of parameters can be large, resulting in poor forecast accuracy. To decrease the number of parameters, we use the varying coefficient model, in which the coefficients are expressed as a smooth function of the time interval.

Under the above considerations, we propose expressing b_{ij} as follows:

$$b_{ij} = \sum_{m=1}^M \beta_m(j) g_m(\mathbf{s}_i), \quad (3)$$

where $g_m(\mathbf{s}_i)$ ($m = 1, \dots, M$) are basis functions given beforehand, $\beta_m(j)$ are functions of regression coefficients, and M is the number of basis functions.

We also use the basis expansion for $\beta_m(j)$:

$$\beta_m(j) = \sum_{q=1}^Q \gamma_{qm} h_q(j), \quad (4)$$

where $h_q(j)$ ($q = 1, \dots, Q$) are basis functions given beforehand and γ_{qm} are the elements of the coefficient matrix $\mathbf{\Gamma} = (\gamma_{qm})$. Substituting (4) into (3) results in the following:

$$b_{ij} = \sum_{m=1}^M \sum_{q=1}^Q \gamma_{qm} h_q(j) g_m(\mathbf{s}_i). \quad (5)$$

Because $h_q(j)$ and $g_m(\mathbf{s}_i)$ are known functions, the parameters concerning b_{ij} are γ_{qm} .

Since the effect of weather is assumed to be smooth according to both j and \mathbf{s}_i , we use basis functions $h_q(j)$ and $g_m(\mathbf{s}_i)$, which produce a smooth function, such as B-spline and the radial basis function (RBF).

2.2 Expression of μ_{ij}

Since μ_{ij} is the effect of past consumption, one can assume that μ_{ij} is expressed as a linear combination of past consumption $y_{(i-t-L_\alpha)j}$, i.e.,

$$\mu_{ij} = \sum_{t=1}^T \alpha_{jt} y_{(i-t-L_\alpha)j} + \sum_{u=1}^U \beta_{ju} y_{i(j-u-L_\beta)}, \quad (6)$$

where T and U are positive integers, which denote how far we trace back through the data and α_{jt} ($t = 1, \dots, T$) and β_{ju} ($u = 1, \dots, U$) are positive values given beforehand. Here, L_α and L_β are nonnegative integers that describe the lags; these values change according to the closing time of transactions*. The regression coefficients α_{jt} correspond to the effects of past consumptions for the same time interval on previous days, while β_{jt} are the coefficients for different time intervals on the same day. For the day-ahead market, we assume that $\beta_{ju} \equiv 0$.

In practice, however, it is assumed that past consumption also depends on past weather, such as daily temperature. For example, suppose that it was exceptionally hot yesterday and it is cooler today. In this case, it is not desirable to directly use past consumption as the predictor; it is better to remove the effect of past temperature from past consumption. In other words, we can use $y_{(i-t-L_\alpha)j} - b_{(i-t-L_\alpha)j}$ and $y_{i(j-u-L_\beta)} - b_{i(j-u-L_\beta)}$ instead of $y_{(i-t-L_\alpha)j}$, and $y_{i(j-u-L_\beta)}$, respectively. As a result, μ_{ij} is expressed as follows:

$$\mu_{ij} = \sum_{t=1}^T \alpha_{jt} (y_{(i-t-L_\alpha)j} - b_{(i-t-L_\alpha)j}) + \sum_{u=1}^U \beta_{ju} (y_{i(j-u-L_\beta)} - b_{i(j-u-L_\beta)}). \quad (7)$$

Substituting (7) into (5) results in the following:

$$\begin{aligned} \mu_{ij} = & \sum_{t=1}^T \alpha_{jt} y_{(i-t-L_\alpha)j} - \sum_{t=1}^T \sum_{m=1}^M \sum_{q=1}^Q \alpha_{jt} \gamma_{qm} h_q(j) g_m(\mathbf{s}_{i-t-L_\alpha}) \\ & + \sum_{u=1}^U \beta_{ju} y_{i(j-u-L_\beta)} - \sum_{u=1}^U \sum_{m=1}^M \sum_{q=1}^Q \beta_{ju} \gamma_{qm} h_q(j-u-L_\beta) g_m(\mathbf{s}_i). \end{aligned} \quad (8)$$

The appropriate values of α_{jt} and β_{ju} are chosen by several approaches. A simple method is $\alpha_{jt} = 1/T$ and $\beta_{ju} = 1/U$, which implies μ_{ij} is the sample mean of the

*For example, transactions of the day-ahead market in the JEPX close at 5:00 pm every day. For the forecast of the 5:30–6:00 pm interval tomorrow, we cannot use the information of today's consumption at the 5:30–6:00 pm interval due to the trading hours of the market, which implies $L_\alpha = 1$.

past consumption. Another method is based on the AR(1) structure, i.e., $\alpha_{jt} = \rho_\alpha^t$ and $\beta_{ju} = \rho_\beta^u$, where ρ_α and ρ_β satisfy $\sum_{t=1}^T \rho_\alpha^t = 1$ and $\sum_{u=1}^U \rho_\beta^u = 1$, respectively. Note that $\sum_{t=1}^T \rho^t = \rho(1 - \rho^T)/(1 - \rho)$, so $\sum_{t=1}^T \rho^t = 1$ is equivalent to $\rho^{T+1} - 2\rho + 1 = 0$, whose numerical solution is easily obtained.

2.3 Proposed model

By combining the expressions of b_{ij} in (5) and μ_{ij} in (8), the model (2) is expressed as follows:

$$\begin{aligned}
y_{ij} = & \frac{1}{T} \sum_{t=1}^T y_{(i-t-L_\alpha)j} - \frac{1}{T} \sum_{t=1}^T \sum_{m=1}^M \sum_{q=1}^Q \gamma_{qm} h_q(j) g_m(\mathbf{s}_{i-t-L_\alpha}) \\
& + \frac{1}{U} \sum_{u=1}^U y_{i(j-u-L_\beta)} - \frac{1}{U} \sum_{u=1}^U \sum_{m=1}^M \sum_{q=1}^Q \gamma_{qm} h_q(j-u-L_\beta) g_m(\mathbf{s}_i) \\
& + \sum_{m=1}^M \sum_{q=1}^Q \gamma_{qm} h_q(j) g_m(\mathbf{s}_i) + \varepsilon_{ij}.
\end{aligned} \tag{9}$$

The model (9) is equivalent to the linear regression model

$$\tilde{\mathbf{y}} = \mathbf{X}\boldsymbol{\gamma} + \boldsymbol{\varepsilon}, \tag{10}$$

where $\boldsymbol{\gamma} = \text{vec}(\boldsymbol{\Gamma})$ and $\boldsymbol{\varepsilon} = \text{vec}(\mathbf{E})$ with $\mathbf{E} = (\varepsilon_{ij})$. Here, \mathbf{X} and $\tilde{\mathbf{y}}$ are considered as the design matrix and the response vector, respectively. The definitions of $\tilde{\mathbf{y}}$ and \mathbf{X} are given in Appendix A.

Remark 2.1. Although this study considers a statistical model that can be applied to the electricity markets (i.e., 30-minute intervals), our proposed model is directly applicable to any time resolution of data; for example, the load in 1-minute intervals and temperature in 1-hour intervals.

3 Estimation

3.1 Nonnegative least squares

To estimate the regression coefficient vector $\boldsymbol{\gamma}$, one can use the least squares estimation (LSE)

$$\min_{\boldsymbol{\gamma}} \|\tilde{\mathbf{y}} - \mathbf{X}\boldsymbol{\gamma}\|_2^2.$$

In our experience, however, the elements of least squares estimates $\hat{\gamma}$ often become negative. In such cases, the estimate of b_{ij} is negative because the basis functions $h_q(j)$ and $g_m(\mathbf{s}_i)$ are generally positive values. When $b_{ij} < 0$, the values of μ_{ij} become extremely large to adjust for the negative b_{ij} value, which makes interpreting the estimated model difficult. Indeed, $y_{ij} \approx \mu_{ij} + b_{ij}$ means the current consumption is decomposed by the effect of past consumption and that of weather. The interpretation may be realized only when b_{ij} is a nonnegative value; in that case, the value of b_{ij} implies how the weather affects the loads.

A nonnegative value of the weather effect b_{ij} is realized when all elements of γ are nonnegative. The nonnegative least squares (NNLS) estimation is useful for estimating nonnegative regression coefficients:

$$\min_{\gamma} \|\tilde{\mathbf{y}} - \mathbf{X}\gamma\|_2^2 \quad \text{subject to } \gamma \geq \mathbf{0}. \quad (11)$$

The optimization problem (11) is a special case of quadratic programming with nonnegativity constraints (e.g., Franc et al., 2005). As a result, the NNLS problem becomes a convex optimization problem. Several efficient algorithms to obtain the solution in (11) have been proposed in the literature (e.g., Lawson and Hanson, 1995; Bro and DeJong, 1997; Timotheou, 2016).

We add the ridge penalty (Hoerl and Kennard, 1970) to the loss function of the NNLS estimation:

$$\min_{\gamma} \|\tilde{\mathbf{y}} - \mathbf{X}\gamma\|_2^2 + \lambda\|\gamma\|_2^2 \quad \text{subject to } \gamma \geq \mathbf{0}, \quad (12)$$

where $\lambda > 0$ is a regularization parameter. In our experience, the ridge penalization yields a stable estimator and improves the forecast accuracy.

3.2 Forecast

For the day-ahead forecast, we forecast the loads on the next day, $\hat{y}_{(i+1)j}$, for the given NNLS estimate $\hat{\gamma}$ and weather information \mathbf{s}_{i+1} . The forecast value $\hat{y}_{(i+1)j}$ is expressed as follows:

$$\hat{y}_{(i+1),j} = \hat{\mu}_{(i+1)j} + \hat{b}_{(i+1)j}$$

Here, $\hat{b}_{(i+1)j} = \sum_{m=1}^M \sum_{q=1}^Q \hat{\gamma}_{qm} h_q(j) g_m(\mathbf{s}_{i+1})$ and $\hat{\mu}_{(i+1)j} = \sum_{t=1}^T \alpha_{jt} (y_{(i+1-t-L_\alpha)j} - \hat{b}_{(i+1-t-L_\alpha)j})$.

On the intraday forecast, we may use information about the loads on that day so that $\hat{\mu}_{(i+1)j}$ is expressed as

$$\hat{\mu}_{(i+1)j} = \sum_{t=1}^T \alpha_{jt} (y_{(i+1-t-L_\alpha)j} - \hat{b}_{(i+1-t-L_\alpha)j}) + \sum_{u=1}^U \beta_{ju} (y_{(i+1)(j-u-L_\beta)} - \hat{b}_{(i+1)(j-u-L_\beta)}).$$

Construction of a forecast interval based on (11) or (12) is not easy due to the constraints of the parameter. To derive the forecast interval, we employ a two-stage procedure; first, we estimate the parameter via NNLS to extract variables that correspond to nonzero coefficients. Then, we employ the least squares estimation based on the variables selected in the first step. With this procedure, we should derive the forecast interval after model selection. To achieve this result, the post-selection inference (Lee and Taylor, 2014; Lee et al., 2016) is employed. The post-selection inference for the NNLS estimation is detailed in Appendix B.

4 Case study

4.1 Data

The performance of our proposed procedure is investigated through analysis of electricity load data collected at a research facility. The dataset consists of electricity loads from January 4th, 2016, to December 31st, 2018. The loads are shown in kWh at 30-minute intervals (i.e., $J = 48$). At certain times, loads are not observed due to electricity meter failures or blackouts. When some data values are missing for a particular day, the data for that day are removed, resulting in 1061 days of complete data.

We use maximum temperature around the research facility as weather variables \mathbf{s}_i . We consider the problem of the day-ahead forecast: $\beta_{ju} \equiv 0$. To eliminate the effect of the day of the week, the statistical models are constructed by day of the week; thus, we produce seven statistical models. All national holidays are regarded as Sundays, and we forecast the loads from January 2017 to December 2018 (the data in 2016 are only used for training). The training data consist of all load data up to the previous day of the forecast day; for example, when we forecast the loads on February 4th, 2017, the training

data are loads from January 4th, 2016, to February 3rd, 2017.

The research facility has experimental equipment that uses large amounts of electricity, and the usage schedule of the experimental equipment is irregular. For this reason, we exclude the loads of the experimental equipment from the forecast loads of the research facility.

4.2 Setting

We compare the performance of our proposed methods based on various settings:

- Two types of α_{jt} : $\alpha_{jt} = 1/T$ (hereafter referred to as “ $\alpha 1$ ”) and AR(1) structure (hereafter referred to as “ $\alpha 2$ ”). Details of the AR(1) structure are presented at the end of Section 2.2.
- Two estimation procedures: ridge estimation

$$\min_{\boldsymbol{\gamma}} \|\tilde{\boldsymbol{y}} - \mathbf{X}\boldsymbol{\gamma}\|_2^2 + \lambda \|\boldsymbol{\gamma}\|_2^2$$

and NNLS with the ridge penalty in (12). We label these estimation procedures “E1” and “E2”, respectively.

- Two types of mean structures: $\mu_{ij} = \sum_{t=1}^T \alpha_{jt}(y_{(i-t)j} - \mu_{(i-t)j})$ in (7) and $\mu_{ij} = \sum_{t=1}^T \alpha_{jt}y_{(i-t)j}$ in (6). Hereafter, the mean structures $\mu_{ij} = \sum_{t=1}^T \alpha_{jt}(y_{(i-t)j} - \mu_{(i-t)j})$ and $\mu_{ij} = \sum_{t=1}^T \alpha_{jt}y_{(i-t)j}$ are referred to as “ $\mu 1$ ” and “ $\mu 2$ ”, respectively.

The number of settings based on the combination of the above settings is 8. We label these settings as follows: $S_{\alpha 1, E1, \mu 1}$, $S_{\alpha 2, E1, \mu 1}$, $S_{\alpha 1, E2, \mu 1}$, $S_{\alpha 2, E2, \mu 1}$, $S_{\alpha 1, E1, \mu 2}$, $S_{\alpha 2, E1, \mu 2}$, $S_{\alpha 1, E2, \mu 2}$, and $S_{\alpha 2, E2, \mu 2}$.

For the basis function $g_m(\mathbf{s}_i)$, we use the radial basis function (RBF) with a hyperparameter $\nu_g > 0$ (Ando et al., 2008):

$$g_m(\mathbf{x}; \boldsymbol{\mu}_m, h_m) = \exp\left(-\frac{\|\mathbf{x} - \boldsymbol{\mu}_m\|^2}{2\nu_g h_m^2}\right),$$

where $\boldsymbol{\mu}_m$ and h_m^2 are mean vector and variance, respectively, for the m th cluster. To determine $\boldsymbol{\mu}_m$ and h_m^2 , we employ a two-stage procedure given by Moody and Darken

(1989). First, we apply k -means clustering to $\mathbf{s}_1, \dots, \mathbf{s}_n$ and obtain clusters $\{C_1, \dots, C_M\}$. Then, $\boldsymbol{\mu}_m$ and h_m^2 are estimated as follows:

$$\hat{\boldsymbol{\mu}}_m = \frac{1}{\#C_m} \sum_{\mathbf{s}_i \in C_m} \mathbf{s}_i, \quad \hat{h}_m^2 = \frac{1}{\#C_m} \sum_{\mathbf{s}_i \in C_m} (\mathbf{s}_i - \hat{\boldsymbol{\mu}}_m)^2,$$

where $\#C_m$ is the number of observations in cluster C_m . The basis function $h_q(j)$ is constructed the same way as shown above, but the coefficient function $\beta_m(j)$ is not continuous around the boundary (e.g., $j = 1, 48$) with the ordinary RBF. To obtain a continuous function, we slightly modify the RBF function as follows:

$$h_q(j; \eta_q, \zeta_q) = \sum_{k=0, \pm 1, \pm 2} \exp \left\{ -\frac{(j + Jk - \eta_q)^2}{2\nu_h \zeta_q^2} \right\}.$$

For each setting, we prepare 180 patterns of tuning parameters: $Q = 5, 10$, $M = 5, 10$, $T = 4$, $\nu_g = 1, 4, 9$, $\nu_h = 1, 4, 9$, and $\lambda = 0, 10^{-8}, 10^{-6}, 10^{-4}, 10^{-2}$. These tuning parameters are chosen so that the root mean squared error (RMSE)

$$\text{RMSE} = \sqrt{\frac{1}{Jn} \sum_{i=1}^n \sum_{j=1}^J (y_{ij} - \hat{y}_{ij})^2} \quad (13)$$

is minimized.

Table 1 shows a set of tuning parameters selected on the basis of the RMSE. For all settings, the ridge parameter λ is positive, which suggests that the ridge penalty may be helpful for improvement of the forecast accuracy. The optimal values of the tuning parameters depend on the statistical model. For example, by comparing $S_{\alpha 2, E1, \mu 1}$ and $S_{\alpha 2, E2, \mu 1}$, we find that the NNLS estimation results in a more complex model than the LSE ($M = 5$ and $M = 10$ for $S_{\alpha 2, E1, \mu 1}$ and $S_{\alpha 2, E2, \mu 1}$, respectively); due to the constraints on the parameters of the NNLS estimation, the NNLS estimation may require more parameters than the LSE to obtain good forecast accuracy.

4.3 Evaluation

We evaluate the performance of our proposed method through the monthly mean absolute percentage error (MAPE)

$$\text{MAPE} = \frac{1}{Jn} \sum_{i=1}^n \sum_{j=1}^J \frac{|y_{ij} - \hat{y}_{ij}|}{y_{ij}}. \quad (14)$$

Table 1: Set of tuning parameters that result in minimum RMSE.

	$S_{\alpha 1, E1, \mu 1}$	$S_{\alpha 2, E1, \mu 1}$	$S_{\alpha 1, E2, \mu 1}$	$S_{\alpha 2, E2, \mu 1}$	$S_{\alpha 1, E1, \mu 2}$	$S_{\alpha 2, E1, \mu 2}$	$S_{\alpha 1, E2, \mu 2}$	$S_{\alpha 2, E2, \mu 2}$
Q	10	10	10	10	10	10	10	5
M	5	5	10	10	5	5	10	10
ν_g	9	9	9	9	1	1	4	4
ν_h	9	4	4	4	1	1	1	9
λ	10^{-4}	10^{-4}	10^{-4}	10^{-4}	10^{-2}	10^{-2}	10^{-4}	10^{-2}

The results are shown in Table 2. For all methods, the forecast error is relatively high. This result occurs because the research facility is small and the electricity usage is unstable. As seen later, standard machine learning techniques also result in high forecast error. We observe that setting $\mu 1$ generally performs better than setting $\mu 2$ during seasonal changes, such as those during July 2017 and March and September 2018. The effect of past loads shown by model $\mu 1$ may appropriately remove the past temperature effect. The performance of the NNLS estimation (E2) is comparable with that of the LSE (E1), which suggests that restricting the regression coefficients to all positive values may not cause a significant decrease in forecast accuracy. For setting $\mu 1$, the performance of $\alpha 1$ is similar to that of $\alpha 2$. On the other hand, for setting $\mu 2$, sometimes $\alpha 1$ results in a much worse performance than $\alpha 2$, especially during seasonal changes. The use of old loads, such as loads from 28 (=7·4) days ago, may decrease the forecast accuracy because the load patterns may change for several tens of days during seasonal changes.

In March 2018, the forecast errors are large due to seasonal changes. To investigate the performance in detail, we show the forecast values and actual values of loads from March 1st to 12th, 2018, in Figure 1. For setting $\mu 2$, the forecast values are often larger than the actual values; thus, setting $\mu 2$ cannot appropriately capture the effect of temperature. Indeed, the past loads in February are generally larger than those in March, as shown in Figure 2; in Japan, it is much colder in February than in March. For example, to forecast the loads on March 5th, we use the past loads of the past four days of the same weekday: January 29th and February 5th, 19th, and 26th (February 12th was a national holiday in Japan and regarded as Sunday). The loads on the past four days are much larger than that on March 5th. The maximum temperatures on these five days (past four

Table 2: Monthly mean average error (MAE) for our proposed methods.

	$S_{\alpha_1, E1, \mu_1}$	$S_{\alpha_2, E1, \mu_1}$	$S_{\alpha_1, E2, \mu_1}$	$S_{\alpha_2, E2, \mu_1}$	$S_{\alpha_1, E1, \mu_2}$	$S_{\alpha_2, E1, \mu_2}$	$S_{\alpha_1, E2, \mu_2}$	$S_{\alpha_2, E2, \mu_2}$
17, Jan	15.4	15.8	15.1	16.6	16.7	17.2	15.2	15.9
17, Feb	7.2	7.7	7.6	8.3	7.8	7.3	8.8	8.4
17, Mar	7.4	6.7	7.5	6.9	6.5	5.5	9.0	7.2
17, Apr	5.9	4.9	6.4	5.4	4.9	4.6	6.7	5.5
17, May	11.3	11.5	11.2	11.6	13.5	13.1	12.1	12.1
17, Jun	8.8	8.4	9.4	8.7	8.6	8.4	8.6	8.5
17, Jul	15.3	15.9	17.1	17.4	21.4	19.7	19.5	18.1
17, Aug	14.1	13.9	13.9	13.7	17.0	16.1	18.3	17.4
17, Sep	7.7	7.5	9.2	8.3	17.4	13.8	18.8	14.8
17, Oct	5.5	5.5	5.5	5.3	6.5	6.1	7.3	6.5
17, Nov	7.2	7.1	7.5	7.5	9.6	9.6	8.3	8.4
17, Dec	13.5	14.0	13.6	14.2	19.1	17.9	18.1	17.1
18, Jan	14.3	14.5	15.8	15.8	14.7	14.5	13.6	13.5
18, Feb	9.6	9.3	10.0	9.8	13.7	13.3	13.5	13.4
18, Mar	13.7	12.6	14.3	12.9	23.2	17.3	26.4	19.7
18, Apr	7.6	6.8	7.6	6.6	9.0	7.9	8.6	6.9
18, May	12.3	12.3	12.7	12.8	15.5	14.7	13.5	13.4
18, Jun	13.9	11.9	14.0	12.0	15.6	12.7	14.1	11.7
18, Jul	7.7	8.2	8.2	8.7	10.5	10.4	9.1	9.6
18, Aug	6.9	6.8	7.3	7.2	7.6	7.1	7.6	7.3
18, Sep	8.7	9.6	10.1	10.4	19.5	17.6	21.1	18.7
18, Oct	7.4	6.7	7.7	6.7	14.0	10.5	16.8	12.0
18, Nov	10.9	10.5	10.6	10.3	15.5	13.9	12.5	11.7
18, Dec	10.7	10.0	11.0	10.3	12.2	11.5	11.2	10.8

days and March 5th) are shown in Table 3 to investigate the relationship between load and temperature. Table 3 shows that the temperature on March 5th is much higher than that on the past four days. Therefore, without removing the effect of temperature from past loads, the forecast on March 5th may not work accurately.

The estimated model can be interpreted by decomposing the forecast value by the effects of temperature and past loads: $\hat{g}_{ij} = \hat{b}_{ij} + \hat{\mu}_{ij}$. The values \hat{b}_{ij} and $\hat{\mu}_{ij}$ are depicted

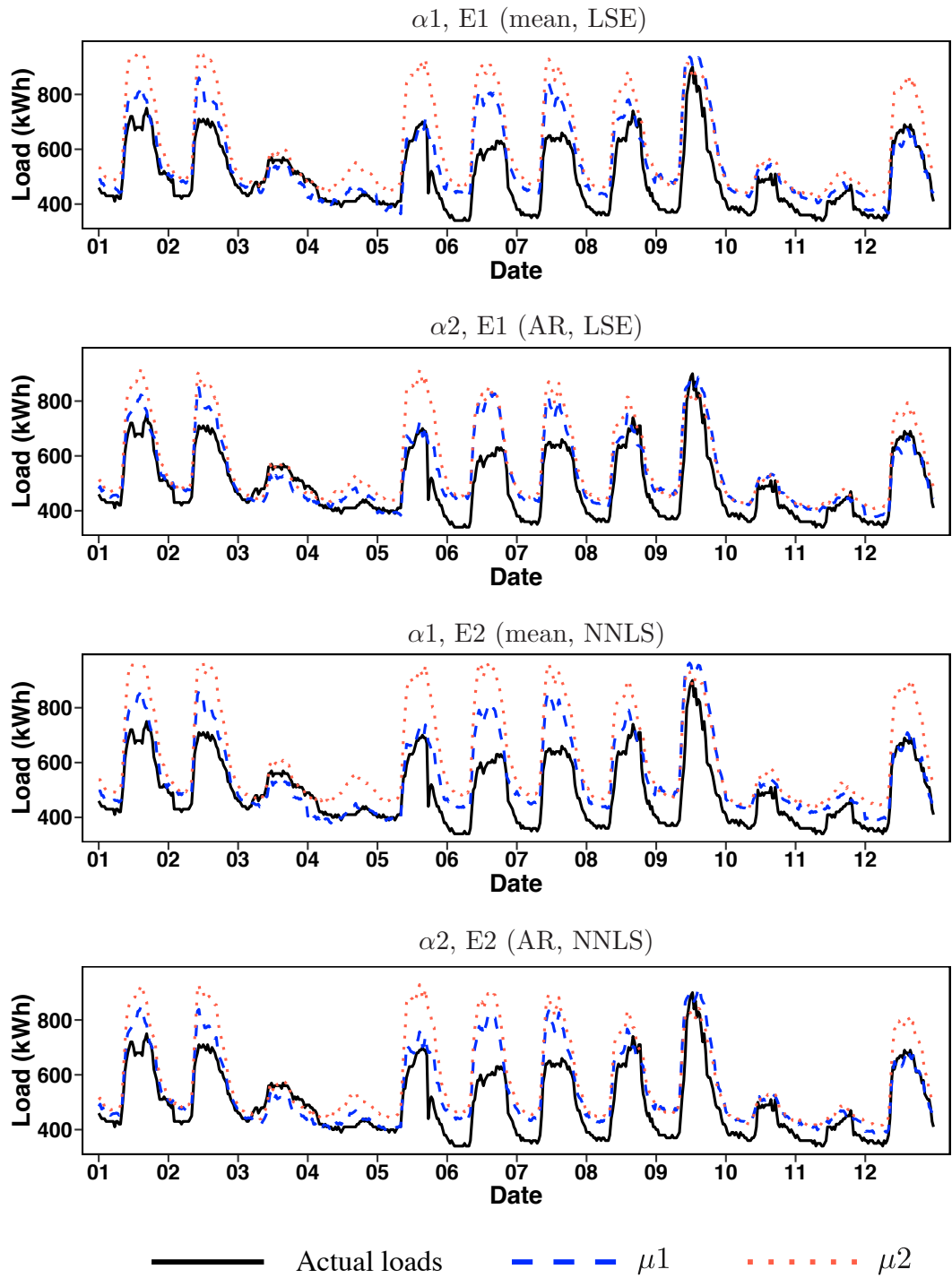


Figure 1: Forecast values and actual values of loads from March 1st to 12th, 2018.

in Figure 3. Because the performances between α_1 and α_2 are similar, we only depict the result for model α_2 . For mean structure μ_2 , the value of \hat{b}_{ij} results in almost 0:

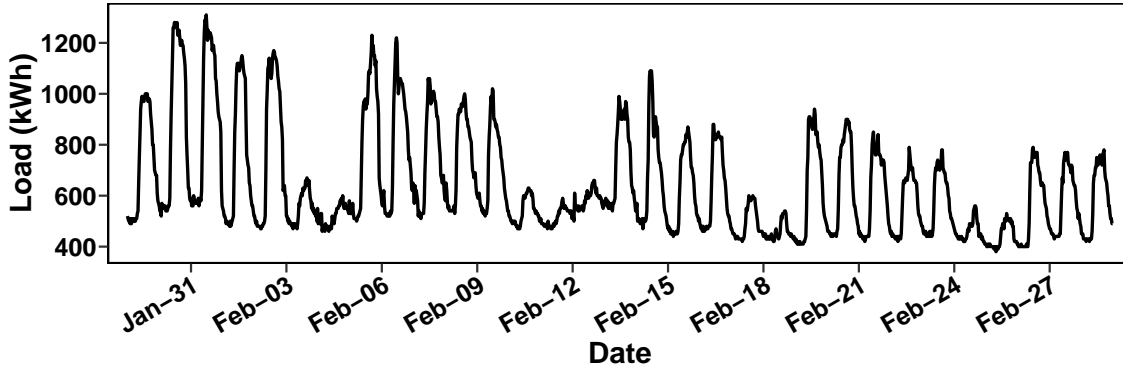


Figure 2: Actual loads from January 29th to February 28th, 2018.

Table 3: Temperatures on several dates in 2018.

Date	Jan 29th	Feb 5th	Feb 19th	Feb 26th	Mar 5th
Temperature	4.3	1.1	10.3	12.6	18.4

$\hat{\mu}_{ij} = \sum_{t=1}^T \alpha_{jt} y_{(i-t)j}$ may not appropriately capture the effect of temperature. The poor performance on March 5th by model μ_2 is attributed to the above fact. On the other hand, for model μ_1 , \hat{b}_{ij} may appropriately capture the effect of temperature.

Although the forecast accuracy of the LSE is similar to that of the NNLS estimation, the results of the decomposition $\hat{y}_{ij} = \hat{b}_{ij} + \hat{\mu}_{ij}$ are completely different. The LSE often results in negative values of \hat{b}_{ij} , and then $\hat{\mu}_{ij}$ becomes much larger than the actual load. Thus, interpreting the effect of weather is difficult with the LSE. This issue occurs because there are no restrictions on the sign of \hat{b}_{ij} . On the other hand, the effect of weather is appropriately captured by the NNLS estimation. For example, on March 5th, the effect of the weather is small due to the moderate temperature on that day; on the other hand, the LSE results in large negative values for \hat{b}_{ij} . The constraint on nonnegativeness of γ greatly improves the interpretation of the estimated model.

To further investigate the effect of temperature, we depict \hat{b}_{ij} when maximum temperatures are 5°C (cold day), 20°C (cool day), and 35°C (hot day), which is shown in Figure 4. Because we estimate the parameter for each day of the week separately, the weather effects b_{ij} differ by the day of the week. We depict \hat{b}_{ij} on Tuesday and Sunday. The parameter γ is estimated by using the loads from January 4th, 2016, to December 31st, 2018. The estimation procedure uses setting S_{α_2, E_2, μ_1} and “separate regression”,

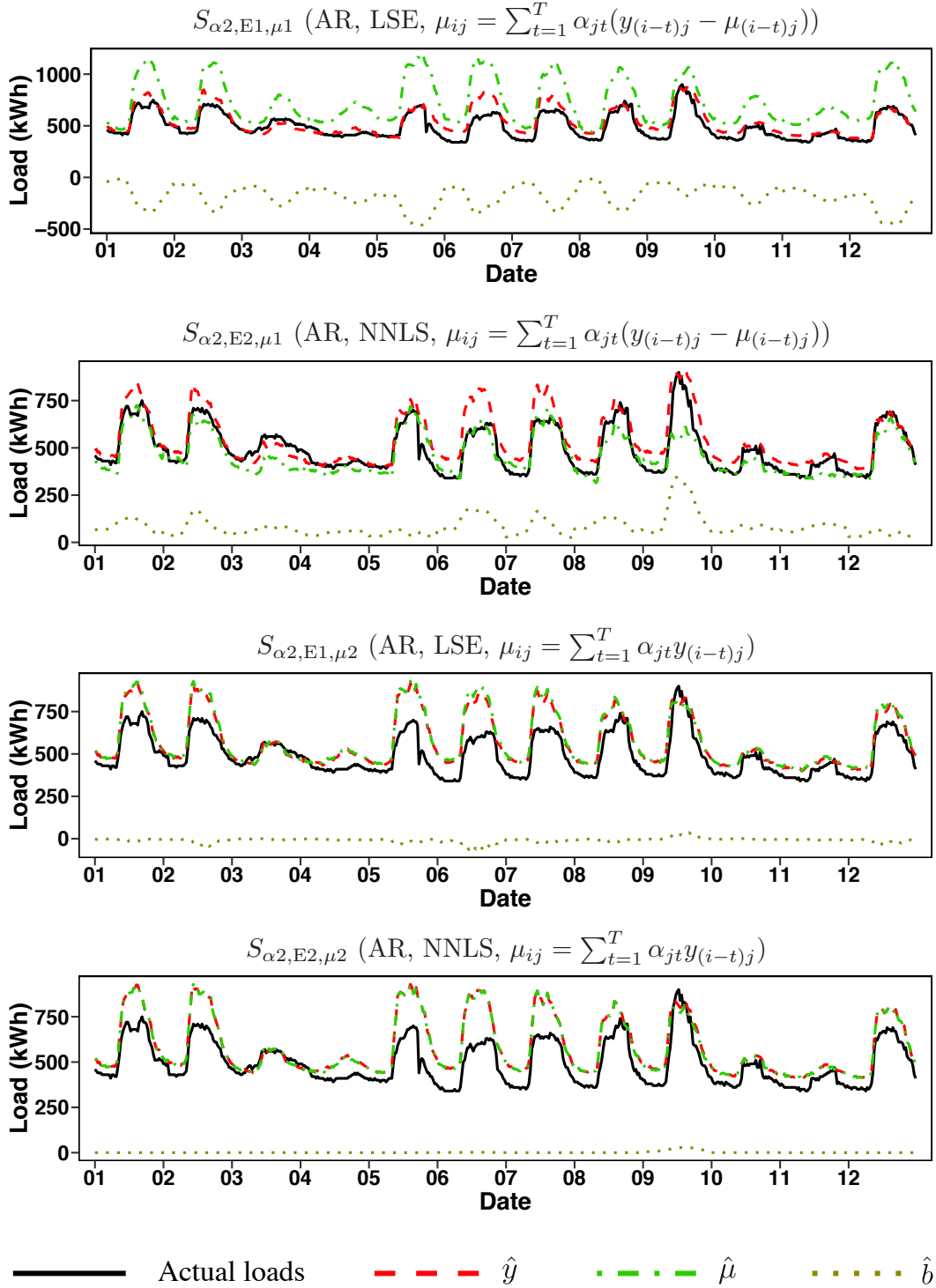


Figure 3: The values \hat{b}_{ij} and $\hat{\mu}_{ij}$ from March 1st to 12th, 2018.

where the regression is conducted for each time interval separately. The results of our proposed procedure show that \hat{b}_{ij} is highly dependent on the temperature: the weather

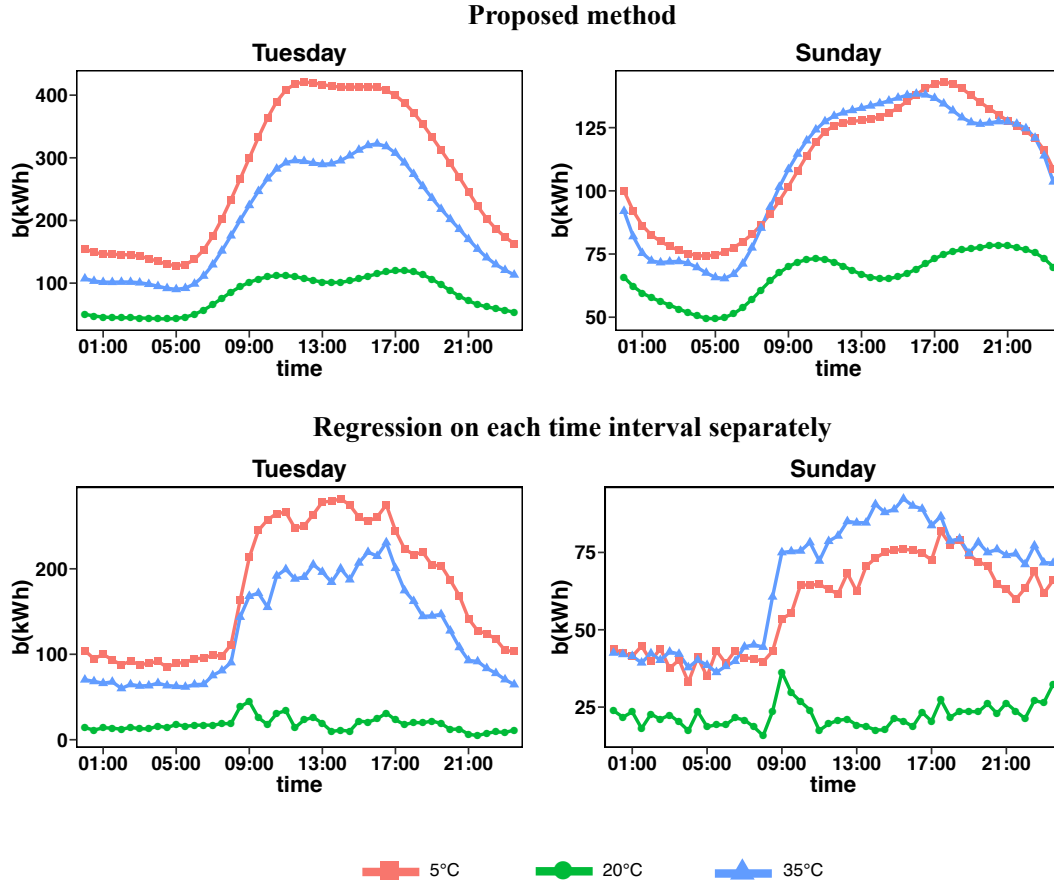


Figure 4: The weather effect b_{ij} on Tuesday and Sunday. The parameter γ is estimated by using the dataset from January 4th, 2016, to December 31st, 2018. The estimation procedure uses setting S_{α_2, E_2, μ_1} (upper side) and “separate regression”, where the regression is conducted for each time interval separately (lower side).

effect may be large for cold and hot days due to air conditioner use. Moreover, the weather effect on Tuesday is generally more significant than that on Sunday because Tuesday is a working day while Sunday is a weekend day at this research facility. When we conduct the regression analysis for each time interval separately, the daily curve of \hat{b}_{ij} becomes non-smooth. As a result, our proposed method is more appropriate for interpreting the weather effect than the separate regression. Note that even if we increase the value of the ridge parameter, the weather effect of the separate regression remains non-smooth in our experience. Therefore, a smooth function for regression coefficients is essential for producing a smooth curve for \hat{b}_{ij} .

4.4 Comparison with standard machine learning techniques

We compare the performance of our proposed method with the following popular machine learning techniques: random forest, support vector regression (SVR), and lasso. The predictors are electricity loads of the past $T = 4$ days and maximum temperature. We use R packages `randomForest`, `ksvm`, and `glmnet` to implement these machine learning techniques. In SVR, we use the Gaussian Kernel. The SVR includes several tuning parameters; σ is used in the Gaussian Kernel, C corresponds to the regularization parameter in the SVR problem, and ϵ is used in the regression. The data in ϵ -tube around the prediction value is not penalized. We prepare the candidates $\sigma = 0.001, 0.01, 0.1$, $C = 1, 10, 100$ and $\epsilon = 0.001, 0.01, 0.1$. The tuning parameters of random forest include the number of trees n_{trees} and the number of variables sampled at each split, say n_{var} . The candidates of these parameters are $n_{trees} = 50, 100, 500$ and $n_{var} = 1, 2, 3$. In the lasso, the candidates of regularization parameter λ are set as follows: maximum and minimum values of λ are defined by $\lambda_{\max} = 200$ and $\lambda_{\min} = 0.01$, respectively, and 100 grids are constructed on a log scale. We choose tuning parameters that yield the smallest value of RMSE in (13).

Table 4 shows the MAPE given by (14) for our proposed methods and machine learning techniques. Among all methods, $S_{\alpha 2, E1, \mu 1}$ yields the best performance in terms of MAPE. $S_{\alpha 2, E2, \mu 1}$ performs slightly worse than but comparable with $S_{\alpha 2, E1, \mu 1}$. If an interpretation of the estimated model is needed, $S_{\alpha 2, E2, \mu 1}$ is better than $S_{\alpha 2, E1, \mu 1}$. Both $S_{\alpha 2, E1, \mu 1}$ and $S_{\alpha 2, E2, \mu 1}$ perform slightly better than the machine learning techniques. The forecast accuracy of the machine learning techniques might be improved when we include more information about weather and past loads (e.g., Khoshrou and Pauwels, 2019). However, even if the forecast accuracy is improved, the standard machine learning techniques cannot provide a smooth curve for \hat{b}_{ij} .

5 Concluding remarks

We have constructed a statistical model for forecasting future electricity loads. The key idea of our proposed model is decomposition of the load expressed as $y_{ij} \approx b_{ij} + \mu_{ij}$,

Table 4: Mean absolute percentage error (MAPE) for various methods from 2017 to 2018.

$S_{\alpha 1, E1, \mu 1}$	$S_{\alpha 2, E1, \mu 1}$	$S_{\alpha 1, E2, \mu 1}$	$S_{\alpha 2, E2, \mu 1}$	$S_{\alpha 1, E1, \mu 2}$	$S_{\alpha 2, E1, \mu 2}$	$S_{\alpha 1, E2, \mu 2}$	$S_{\alpha 2, E2, \mu 2}$
10.4	10.1	10.6	10.4	13.4	12.3	13.2	12.0

SVR	Random Forest	Lasso
10.9	11.2	11.5

where b_{ij} and μ_{ij} are the effects of weather and past loads, respectively. To capture the nonlinear effect of weather information, we employed the varying coefficient model. Numerical results showed that our method appropriately captured the weather effect and performed slightly better than the standard machine learning techniques. With the ordinary least squares estimation (LSE), the estimate of b_{ij} , say \hat{b}_{ij} , became negative because some of the elements of regression coefficients $\hat{\gamma}$ were negative. The negative weather effect caused interpretation of the estimated model to be difficult. To address this issue, we employed the NNLS estimation; this estimation is performed under the constraint that all of the elements of $\hat{\gamma}$ are nonnegative. The numerical result showed that the NNLS estimation produced a more interpretable model than the LSE. Estimating the amount of electricity fluctuations caused by weather in Figure 4 would be helpful for making strategies for energy-saving intervention and demand response.

The proposed method is carried out under the assumption that the errors are uncorrelated. In practice, however, the errors among near time intervals may be correlated. As a future research topic, it would be interesting to assume a correlation among time intervals and estimate a regression model that includes the correlation parameter.

Acknowledgements

The author would like to thank Professor Hiroki Masuda and Dr. Maiya Hori for helpful comments and discussions. This work was partially supported by the Japan Society for the Promotion of Science KAKENHI 19K11862 and the Center of Innovation Program (COI) from JST, Japan.

Appendix A Matrix notation of our proposed regression model

To show that our proposed model (9) is a regression model, we denote the following:

$$\begin{aligned}
\check{y}_{ij\alpha} &= \sum_{t=1}^T \alpha_{jt} y_{(i-t-L_\alpha)j}, \\
\check{y}_{ij\beta} &= \sum_{u=1}^U \beta_{ju} y_{(j-u-L_\beta)}, \\
\mathbf{h}(j) &= (h_1(j), \dots, h_Q(j))^T, \\
\check{\mathbf{h}}_j &= \sum_{u=1}^U \beta_{ju} \mathbf{h}(j-u-L_\beta), \\
\mathbf{\Gamma} &= (\gamma_{qm}), \\
\boldsymbol{\gamma} &= \text{vec}(\mathbf{\Gamma}), \\
\check{g}_{m,i} &= \sum_{t=1}^T \alpha_{jt} g_m(\mathbf{s}_{(i-t-L_\alpha)}), \\
\check{\mathbf{g}}_i &= (\check{g}_{1,i}, \dots, \check{g}_{M,i})^T, \\
\mathbf{g}_i &= (g_1(\mathbf{s}_i), \dots, g_M(\mathbf{s}_i))^T.
\end{aligned}$$

The model (9) is then expressed as follows:

$$\begin{aligned}
y_{ij} &= \check{y}_{ij\alpha} - \mathbf{h}(j)^T \mathbf{\Gamma} \check{\mathbf{g}}_i + \check{y}_{ij\beta} - \check{\mathbf{h}}_j^T \mathbf{\Gamma} \mathbf{g}_i + \mathbf{h}(j)^T \mathbf{\Gamma} \mathbf{g}_i + \varepsilon_{ij} \\
&= \check{y}_{ij\alpha} + \check{y}_{ij\beta} + \left\{ \mathbf{g}_i \otimes \mathbf{h}(j) - \check{\mathbf{g}}_i \otimes \mathbf{h}(j) - \mathbf{g}_i \otimes \check{\mathbf{h}}_j \right\}^T \boldsymbol{\gamma} + \varepsilon_{ij}.
\end{aligned}$$

Note that we use the following formula for matrices \mathbf{A} , \mathbf{B} , and \mathbf{C} :

$$\begin{aligned}
\text{vec}(\mathbf{ABC}^T) &= (\mathbf{C} \otimes \mathbf{A}) \text{vec}(\mathbf{B}), \\
(\mathbf{A} \otimes \mathbf{B})^T &= \mathbf{A}^T \otimes \mathbf{B}^T.
\end{aligned}$$

Furthermore, we denote the following:

$$\begin{aligned}
\mathbf{q}_i &= (\check{y}_{i1\alpha} + \check{y}_{i1\beta}, \dots, \check{y}_{iJ\alpha} + \check{y}_{iJ\beta})^T, \\
\tilde{\mathbf{y}}_i &= \mathbf{y}_i - \mathbf{q}_i, \\
\tilde{\mathbf{y}} &= (\tilde{\mathbf{y}}_1^T, \dots, \tilde{\mathbf{y}}_n^T)^T, \\
\mathbf{H} &= (\mathbf{h}(1) \dots, \mathbf{h}(J)), \\
\check{\mathbf{H}} &= (\check{\mathbf{h}}(1), \dots, \check{\mathbf{h}}(J)), \\
\mathbf{L}_i &= (\mathbf{g}_i \otimes \mathbf{H} - \check{\mathbf{g}}_i \otimes \mathbf{H} - \mathbf{g}_i \otimes \check{\mathbf{H}}), \\
\mathbf{L} &= (\mathbf{L}_1, \dots, \mathbf{L}_n)^T,
\end{aligned}$$

Thus, we have a linear regression model (10).

Appendix B Post-selection inference for the NNLS estimation

Appendix B.1 Selection event of NNLS

In this section, $\tilde{\mathbf{y}}$ and $\boldsymbol{\gamma}$ are referred to as \mathbf{y} and $\boldsymbol{\beta}$, respectively, which leads to a standard notation of the linear regression model:

$$\mathbf{y} = \mathbf{X}\boldsymbol{\beta} + \boldsymbol{\varepsilon}.$$

The post-selection inference for the NNLS estimation has already been proposed by Lee and Taylor (2014), but these authors lack a parameter constraint. We have added a constraint on the parameter of the selection event. Let \hat{S} be indices that correspond to variables selected on the basis of the NNLS estimation, i.e., $\hat{S} = \{j \mid \hat{\beta}_j \neq 0\}$. Let $-\hat{S}$ be indices of variables not selected in \hat{S} . The KKT condition in the NNLS estimation (Franc et al., 2005; Chen et al., 2011) is

$$\frac{\partial L(\boldsymbol{\beta}, \boldsymbol{\mu})}{\partial \hat{\boldsymbol{\beta}}} = X^T X \hat{\boldsymbol{\beta}} - X^T \mathbf{y} - \boldsymbol{\mu} = \mathbf{0}, \quad (15)$$

$$\hat{\boldsymbol{\beta}} \geq \mathbf{0}, \quad (16)$$

$$\boldsymbol{\mu} \geq \mathbf{0}, \quad (17)$$

$$\hat{\boldsymbol{\beta}}^T \boldsymbol{\mu} = 0, \quad (18)$$

where $\boldsymbol{\mu}$ is the Lagrange multiplier. Substituting $\hat{\boldsymbol{\beta}} = (\hat{\boldsymbol{\beta}}_{\hat{S}}^T, \hat{\boldsymbol{\beta}}_{-\hat{S}}^T)^T$ into (15) – (18) results in

$$-X_{\hat{S}}^T (\mathbf{y} - X_{\hat{S}} \hat{\boldsymbol{\beta}}_{\hat{S}}) \geq \mathbf{0}, \quad (19)$$

$$-X_{-\hat{S}}^T (\mathbf{y} - X_{\hat{S}} \hat{\boldsymbol{\beta}}_{\hat{S}}) \geq \mathbf{0}, \quad (20)$$

$$\hat{\boldsymbol{\beta}}_{\hat{S}} > \mathbf{0}, \quad (21)$$

$$\hat{\boldsymbol{\beta}}_{-\hat{S}} = \mathbf{0},$$

$$\hat{\boldsymbol{\beta}}_{\hat{S}}^T X_{\hat{S}}^T (\mathbf{y} - X_{\hat{S}} \hat{\boldsymbol{\beta}}_{\hat{S}}) = 0. \quad (22)$$

By combining (19), (21), and (22), we obtain

$$X_{\hat{S}}^T (\mathbf{y} - X_{\hat{S}} \hat{\boldsymbol{\beta}}_{\hat{S}}) = \mathbf{0}. \quad (23)$$

Then, we obtain

$$\hat{\boldsymbol{\beta}}_{\hat{S}} = (X_{\hat{S}}^T X_{\hat{S}})^{-1} X_{\hat{S}}^T \mathbf{y}. \quad (24)$$

Eq. (24) implies the NNLS estimate for the active set coincides with the LSE using the active set. Substituting (24) into (20) and (21) results in

$$-X_{-\hat{S}}^T (\mathbf{I} - X_{\hat{S}} (X_{\hat{S}}^T X_{\hat{S}})^{-1} X_{\hat{S}}^T) \mathbf{y} > \mathbf{0}, \quad (25)$$

$$(X_{\hat{S}}^T X_{\hat{S}})^{-1} X_{\hat{S}}^T \mathbf{y} \geq \mathbf{0}. \quad (26)$$

The selection event constructed by (25) and (26) is expressed as

$$\hat{E}(\mathbf{y}) = \{\mathbf{y} \mid A(\hat{S}) \geq 0\},$$

where $A(\hat{S})$ is given by

$$A(\hat{S}) = \begin{pmatrix} X_{-\hat{S}}^T (\mathbf{I} - X_{\hat{S}} X_{\hat{S}}^\dagger) \\ -X_{\hat{S}}^\dagger \end{pmatrix}.$$

This selection event for the NNLS estimation has already been studied by Lee and Taylor (2014) but Lee and Taylor (2014) did not include the first inequality (25).

Appendix B.2 Distribution of the forecast value after model selection

Suppose that $\mathbf{y} \sim N(\boldsymbol{\mu}, \sigma^2 I)$, and consider the problem of deriving the following distribution:

$$\boldsymbol{\eta}^T \mathbf{y} \mid \{A\mathbf{y} \leq \mathbf{b}\}.$$

Here, $\boldsymbol{\eta}$ is an n -dimensional vector given beforehand. For example, if $\boldsymbol{\eta} = X_{\hat{S}}^{\dagger T} \mathbf{e}_j$, then $\boldsymbol{\eta}^T \mathbf{y} = \hat{\beta}_j$. If

$$\begin{aligned} \mathbf{c} &= \boldsymbol{\eta}(\boldsymbol{\eta}^T \boldsymbol{\eta})^{-1}, \\ \mathbf{z} &= (I_n - \mathbf{c}\boldsymbol{\eta}^T) \mathbf{y}, \end{aligned}$$

then

$$\boldsymbol{\eta}^T \mathbf{y} \mid \{A\mathbf{y} \leq \mathbf{b}, \mathbf{z} = \mathbf{z}_0\} \sim \text{TN}(\boldsymbol{\eta}^T \boldsymbol{\mu}, \sigma^2 \|\boldsymbol{\eta}\|^2, \mathcal{V}^-(\mathbf{z}_0), \mathcal{V}^+(\mathbf{z}_0)),$$

where

$$\mathcal{V}^-(\mathbf{z}) = \max_{j:(A\mathbf{c})_j < 0} \frac{b_j - (A\mathbf{z})_j}{(A\mathbf{c})_j},$$

$$\mathcal{V}^+(\mathbf{z}) = \min_{j:(A\mathbf{c})_j > 0} \frac{b_j - (A\mathbf{z})_j}{(A\mathbf{c})_j}.$$

However, we only observe the distribution of $\boldsymbol{\eta}^T \mathbf{y}$ for a given \mathbf{z} . We consider the marginalization with respect to \mathbf{z} . To explain this result, we consider the distribution of a truncated normal distribution

$$F_{\mu, \sigma^2}^{[a, b]}(x) = \frac{\Phi((x - \mu)/\sigma) - \Phi((a - \mu)/\sigma)}{\Phi((b - \mu)/\sigma) - \Phi((a - \mu)/\sigma)}.$$

Then, we have

$$F_{\boldsymbol{\eta}^T \boldsymbol{\mu}, \sigma^2 \|\boldsymbol{\eta}\|^2}^{[\mathcal{V}^-(\mathbf{z}), \mathcal{V}^+(\mathbf{z})]}(\boldsymbol{\eta}^T \mathbf{y}) \mid \{A\mathbf{y} \leq \mathbf{b}\} \sim U(0, 1),$$

which implies

$$P\left(\frac{\alpha}{2} \leq F_{\boldsymbol{\eta}^T \boldsymbol{\mu}, \sigma^2 \|\boldsymbol{\eta}\|^2}^{[\mathcal{V}^-(\mathbf{z}), \mathcal{V}^+(\mathbf{z})]}(\boldsymbol{\eta}^T \mathbf{y}) \leq 1 - \frac{\alpha}{2} \mid A\mathbf{y} \leq \mathbf{b}\right) = 1 - \alpha.$$

To construct the confidence interval for a given new input \mathbf{x} , we let $\boldsymbol{\eta} = X_{\hat{\mathbf{s}}}^{\dagger T} \mathbf{x}$, and we find L and U , which satisfies the following equation:

$$F_{L, \sigma^2 \|\boldsymbol{\eta}\|^2}^{[\mathcal{V}^-(\mathbf{z}), \mathcal{V}^+(\mathbf{z})]}(\boldsymbol{\eta}^T \mathbf{y}) = \frac{\alpha}{2}, \quad F_{U, \sigma^2 \|\boldsymbol{\eta}\|^2}^{[\mathcal{V}^-(\mathbf{z}), \mathcal{V}^+(\mathbf{z})]}(\boldsymbol{\eta}^T \mathbf{y}) = 1 - \frac{\alpha}{2}.$$

Letting $\mathbf{y}^* = (\mathbf{y}^T, \varepsilon)^T$ with $\varepsilon \sim N(0, \sigma^2)$ and $\boldsymbol{\eta} = (\mathbf{x}^T, 1)^T$, we construct the prediction interval. The algorithm of the post-selection inference for the NNLS estimation procedure is shown in Algorithm 1.

References

- N. Amjady. Short-term hourly load forecasting using time-series modeling with peak load estimation capability. *IEEE Transactions on Power Systems*, 16(3):498–505, Aug. 2001.
- N. Amral, C. S. Ozveren, and D. King. Short term load forecasting using Multiple Linear Regression. In *2007 42nd International Universities Power Engineering Conference*, pages 1192–1198. IEEE, Feb. 2008.

Algorithm 1 Selective inference for NNLS

- 1: Conduct NNLS, and obtain a set of indices for the nonzero coefficients \hat{S} .
 - 2: Calculate $X_{\hat{S}}^{\dagger} = (X_{\hat{S}}^T X_{\hat{S}})^{-1} X_{\hat{S}}^T$.
 - 3: Define the matrix of selection event $A(\hat{S}) = \begin{pmatrix} X_{-\hat{S}}^T (\mathbf{I} - X_{\hat{S}} X_{\hat{S}}^{\dagger}) \\ -X_{\hat{S}}^{\dagger} \end{pmatrix}$.
 - 4: **for** $j = 1, \dots, |\hat{S}|$ **do**
 - 5: Let $\boldsymbol{\eta} = X_{\hat{S}}^{\dagger T} \mathbf{e}_j$.
 - 6: Calculate $\mathbf{c} = \Sigma \boldsymbol{\eta} (\boldsymbol{\eta}^T \Sigma \boldsymbol{\eta})^{-1}$, $\mathbf{z} = (I_n - \mathbf{c} \boldsymbol{\eta}^T) \mathbf{y}$.
 - 7: Calculate $\mathcal{V}^-(\mathbf{z}) = \max_{j:(A\mathbf{c})_j < 0} \frac{-(A\mathbf{z})_j}{(A\mathbf{c})_j}$, $\mathcal{V}^+(\mathbf{z}) = \min_{j:(A\mathbf{c})_j > 0} \frac{-(A\mathbf{z})_j}{(A\mathbf{c})_j}$.
 - 8: Find L and U , which satisfies $F_{L, \boldsymbol{\eta}^T \Sigma \boldsymbol{\eta}}^{[\mathcal{V}^-(\mathbf{z}), \mathcal{V}^+(\mathbf{z})]}(\boldsymbol{\eta}^T \mathbf{y}) = \frac{\alpha}{2}$ and $F_{U, \boldsymbol{\eta}^T \Sigma \boldsymbol{\eta}}^{[\mathcal{V}^-(\mathbf{z}), \mathcal{V}^+(\mathbf{z})]}(\boldsymbol{\eta}^T \mathbf{y}) = 1 - \frac{\alpha}{2}$.
 - 9: **end for**
-

T. Ando, S. Konishi, and S. Imoto. Nonlinear regression modeling via regularized radial basis function networks. *Journal of Statistical Planning and Inference*, 138(11):3616–3633, Nov. 2008.

J. Bedi and D. Toshniwal. Deep learning framework to forecast electricity demand. *Applied Energy*, 238:1312–1326, Mar. 2019.

R. Bro and S. DeJong. A fast non-negativity-constrained least squares algorithm. *Journal of Chemometrics*, 11(5):393–401, 1997.

B. L. Cabrera and F. Schulz. Forecasting Generalized Quantiles of Electricity Demand: A Functional Data Approach. *Journal of the American Statistical Association*, 112(517):127–136, Mar. 2017.

D. Chen, R. P. T. b. o. n. analysis, and 2010. Nonnegativity constraints in numerical analysis. *World Scientific*, pages 109–139, Nov. 2011.

Y. Chen, P. Xu, Y. Chu, W. Li, Y. Wu, L. Ni, Y. Bao, and K. Wang. Short-term electrical load forecasting using the Support Vector Regression (SVR) model to calculate the demand response baseline for office buildings. *Applied Energy*, 195:659–670, June 2017.

- H. Cho, Y. Goude, X. Brossat, and Q. Yao. Modeling and Forecasting Daily Electricity Load Curves: A Hybrid Approach. *Journal of the American Statistical Association*, 108(501):7–21, Mar. 2013.
- E. M. de Oliveira and F. L. C. Oliveira. Forecasting mid-long term electric energy consumption through bagging ARIMA and exponential smoothing methods. *Energy*, 144:776–788, Feb. 2018.
- G. Dudek. Pattern-based local linear regression models for short-term load forecasting. *Electric Power Systems Research*, 130:139–147, Jan. 2016.
- E. E. Elattar, J. Goulermas, and Q. H. Wu. Electric Load Forecasting Based on Locally Weighted Support Vector Regression. *IEEE Transactions on Systems, Man, and Cybernetics, Part C (Applications and Reviews)*, 40(4):438–447, May 2010.
- R. F. Engle, C. W. Granger, J. Rice, and A. Weiss. Semiparametric estimates of the relation between weather and electricity sales. *Journal of the American Statistical Association*, 81(394):310–320, Jan. 1986.
- J. Q. Fan and W. Y. Zhang. Statistical estimation in varying coefficient models. *The Annals of Statistics*, 27(5):1491–1518, Oct. 1999.
- V. Franc, V. Hlavac, and M. Navara. Sequential coordinate-wise algorithm for the non-negative least squares problem. *Computer Analysis of Images and Patterns, Proceedings*, 3691:407–414, 2005.
- Z. Guo, K. Zhou, C. Zhang, X. Lu, W. Chen, and S. Yang. Residential electricity consumption behavior: Influencing factors, related theories and intervention strategies. *Renewable and Sustainable Energy Reviews*, 81:399–412, 2018a.
- Z. Guo, K. Zhou, X. Zhang, and S. Yang. A deep learning model for short-term power load and probability density forecasting. *Energy*, 160:1186–1200, Oct. 2018b.
- A. Harvey and S. J. Kopman. Forecasting Hourly Electricity Demand Using Time-Varying Splines. *Journal of the American Statistical Association*, 88(424):1228–1236, Dec. 1993.

- T. Hastie and R. Tibshirani. Varying-Coefficient Models. *Journal of the Royal Statistical Society Series B-Methodological*, 55(4):757–796, Jan. 1993.
- W. He. Load Forecasting via Deep Neural Networks. *Procedia Computer Science*, 122:308–314, 2017.
- A. E. Hoerl and R. W. Kennard. Ridge Regression: Biased Estimation for Nonorthogonal Problems. *Technometrics*, 12(1):55–67, Feb. 1970.
- T. Hong and S. Fan. Probabilistic electric load forecasting: A tutorial review. *International Journal of Forecasting*, 32(3):914–938, 2016.
- T. Hong, M. Gui, M. E. Baran, and H. L. Willis. Modeling and forecasting hourly electric load by multiple linear regression with interactions. *IEEE PES General Meeting*, pages 1–8, July 2010.
- H. Jiang, Y. Zhang, E. Muljadi, J. J. Zhang, and D. W. Gao. A Short-Term and High-Resolution Distribution System Load Forecasting Approach Using Support Vector Regression With Hybrid Parameters Optimization. *IEEE Transactions on Smart Grid*, 9(4):3341–3350, July 2018.
- A. Khoshrou and E. J. Pauwels. Short-term scenario-based probabilistic load forecasting A data-driven approach. *Applied Energy*, 238:1258–1268, Mar. 2019.
- W. Kong, Z. Y. Dong, Y. Jia, D. J. Hill, Y. Xu, and Y. Zhang. Short-Term Residential Load Forecasting Based on LSTM Recurrent Neural Network. *IEEE Transactions on Smart Grid*, 10(1):841–851, Dec. 2018.
- C. L. Lawson and R. J. Hanson. *Solving Least Squares Problems*. Society for Industrial and Applied Mathematics, 1995. doi: 10.1137/1.9781611971217. URL <https://epubs.siam.org/doi/abs/10.1137/1.9781611971217>.
- C.-M. Lee and C.-N. Ko. Short-term load forecasting using lifting scheme and ARIMA models. *Expert Systems With Applications*, 38(5):5902–5911, May 2011.
- J. D. Lee and J. E. Taylor. Exact Post Model Selection Inference for Marginal Screening. *arXiv.1402.5596*, 2014.

- J. D. Lee, D. L. Sun, Y. Sun, and J. E. Taylor. Exact post-selection inference, with application to the lasso. *The Annals of Statistics*, 44(3):907–927, June 2016.
- B. Liu, J. Nowotarski, T. Hong, and R. Weron. Probabilistic Load Forecasting via Quantile Regression Averaging on Sister Forecasts. *IEEE Transactions on Smart Grid*, 8(2):730–737, Mar. 2017.
- S. M. Lundberg and S.-I. Lee. A unified approach to interpreting model predictions. In *Advances in neural information processing systems*, pages 4765–4774, 2017.
- P. Lusi, K. R. Khalilpour, L. Andrew, and A. Liebman. Short-term residential load forecasting: Impact of calendar effects and forecast granularity. *Applied Energy*, 205:654–669, Nov. 2017.
- N. H. Miswan, R. M. Said, and S. H. H. Anuar. ARIMA with regression model in modelling electricity load demand. *Journal of Telecommunication, Electronic and Computer Engineering*, 8(12):113–116, Jan. 2016.
- J. Moody and C. J. Darken. Fast learning in networks of locally-tuned processing units. *Neural Computation*, 1(2):281–294, June 1989. ISSN 0899-7667. doi: 10.1162/neco.1989.1.2.281.
- M. T. Ribeiro, S. Singh, and C. Guestrin. “Why should I trust you?” Explaining the predictions of any classifier. In *Proceedings of the 22nd ACM SIGKDD international conference on knowledge discovery and data mining*, pages 1135–1144, 2016.
- M. C. Ruiz-Abellón, L. A. Fernández-Jiménez, A. Guillamón, A. Falces, A. García-Garre, and A. Gabaldón. Integration of demand response and short-term forecasting for the management of prosumers demand and generation. *Energies*, 13(1):11, 2020.
- A. Y. Saber and A. K. M. R. Alam. Short term load forecasting using multiple linear regression for big data. In *2017 IEEE Symposium Series on Computational Intelligence (SSCI)*, pages 1–6, Nov 2017. doi: 10.1109/SSCI.2017.8285261.

- S. Timotheou. FAST NON-NEGATIVE LEAST-SQUARES LEARNING in the RANDOM NEURAL NETWORK. *Probability in the Engineering and Informational Sciences*, 30(3):379–402, Jan. 2016.
- D. W. van der Meer, J. Widén, and J. Munkhammar. Review on probabilistic forecasting of photovoltaic power production and electricity consumption. 81(Part 1):1484–1512, Jan. 2018.
- J. Vilar, G. Aneiros, and P. Raña. Prediction intervals for electricity demand and price using functional data. *Electrical Power and Energy Systems*, 96:457–472, Mar. 2018.
- F. Wang, L. Liu, Y. Yu, G. Li, J. Li, M. Shafie-Khah, and J. P. Catalao. Impact analysis of customized feedback interventions on residential electricity load consumption behavior for demand response. *Energies*, 11(4):770, 2018.
- B. Yildiz, J. I. Bilbao, and A. B. Sproul. A review and analysis of regression and machine learning models on commercial building electricity load forecasting. *Renewable and Sustainable Energy Reviews*, 73:1104–1122, June 2017.